Mathematical Sciences
a SpringerOpen Journal

ORIGINAL RESEARCH Open Access

Conformal mapping: Schwarz-Christoffel method for flux-switching PM machines

Esin Ilhan*, Emilia T Motoasca, Johan JH Paulides and Elena A Lomonova

Abstract

Purpose: Flux-switching permanent magnet (FSPM) machines are double salient machines with a high energy density suitable for e-mobility. For a fast design process, machine specialists need easy-to-use motor models. For the FSPM model, analytical methods cost high efforts to create and to improve them. Numerical methods such as the finite element method (FEM) have been extensively studied in the literature with little emphasis given to their alternatives.

Methods: This research shows the implementation of the Schwarz-Christoffel (SC) mapping for the FSPM. With this numerical method, the double salient motor geometry is transformed into a simpler geometry to reduce the model complexity. For the electromagnetic analysis, SC mapping is implemented both as a stand-alone method and as an integrated method with the tooth contour method and the orthogonal field diagram method.

Results: Findings are presented in a comparative analysis for all created models including the finite element method. Results show a very good agreement among the presented models.

Conclusions: The results obtained in this paper show that SC mapping is a good alternative to the FEM. With the provided step-by-step explanation on how to implement SC mapping, the method can be expanded to other electrical machine classes.

Keywords: Conformal mapping, Flux-switching machines, Orthogonal field theory, Schwarz-Christoffel mapping

Introduction

Flux-switching permanent magnet (FSPM) machines come with many theoretical advantages [1,2], but they can have a rather unconventional structure by embodying all its energy sources in the same frame (stator). The double salient structure is a must for machine operation, but it results in a nonuniform airgap. Due to these problems, researchers rely on analytical, numerical or integrated techniques [3-6]. To understand the energy conversion of the FSPM and to have accurate field results, integrated methods are very effective.

This paper shows how to implement the numerical conformal mapping, Schwarz-Christoffel (SC) mapping, as an integrated technique for FSPM modelling. In complex mathematics, conformal mapping is a function used to transform a domain into a simpler structure to decrease computational complexity. Due to its angle-preserving feature, this mapping is widely used in engineering such as in electromagnetism, biomedical engineering, thermodynamics, etc. [7-9]. In this paper, SC mapping is integrated with the analytical tooth contour method (TCM) and with orthogonal field diagrams (OFD) to visualize the electric and magnetic field distributions. They are first explained on a double salient cell structure, which is a simple representation of the FSPM's airgap. Next, the simple model is extended for the 12/10 rotary FSPM in Figure 1. In this paper, TCM implementation for the FSPM is done on the same principles as in [6].

*Correspondence: e.ilhan@tue.nl
Department of Electrical Engineering, Eindhoven University of Technology, Eindhoven, 5612 AZ, The Netherlands

Methods

SC mapping

The SC transformation is an example of conformal mapping, which has been already used in several electromagnetic problems to simplify a nonuniform airgap structure of an electrical machine [10-12]. In SC mapping, the airgap region is represented by a polygon, which is referred to by the number of its *vertices*. For polygons with more than three vertices, the mapping function becomes a parameter problem which can only be solved numerically [13]. To

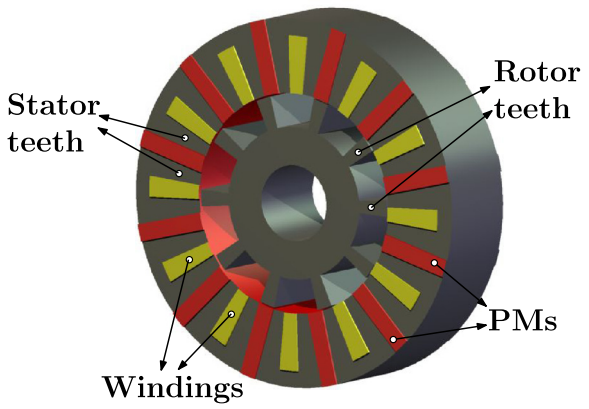

Figure 1 3D illustration of a FSPM with 10 rotor and 12 stator poles.

determine more complex mapping functions, a MATLAB toolbox is available [14].

In the MATLAB SC mapping toolbox, several mapping methods are available for different shapes, e.g. disk, half plane, strip, rectangle, Riemann surfaces, etc. [14]. Regardless of its structure, there are two general rules to describe the polygon:

- The polygon has to be in a quadrilateral shape, i.e. shapes defined in polar coordinates have to be converted to the Cartesian coordinate system.
- The vertices of the polygon have to be defined in a complex plane in a counterclockwise direction.

SC mapping with OFD on a double salient structure

If a harmonic function is mapped with SC to another complex plane, the mapping function is harmonic as well. This feature allows the magnetic and electric potential functions to be uniquely defined in both domains. Using this property and the angle preservation of the conformal maps, OFD can be illustrated by SC mapping as in Figure 2a.

The airgap of a FSPM machine can be represented by a simple double salient cell structure given in Figure 3. In Figure 2a, orthogonal field lines are plotted as equipotential contour lines. Using the SC-OFD method, the electromagnetic behaviour of any region can be analysed in a geometric grid. For the double salient structure, the grid is chosen just below the stator tooth (Figure 3), since the energy conversion takes place here. For two different rotor tooth positions, namely at 20 and 0 mm, the magnetic potential distribution in x-y coordinates of the grid is plotted in Figures 2b and 4c,d. In Figure 4a,b, the stator and rotor teeth are in the aligned position. Figure 4b gives a zoom of the airgap region. In this rotor position, due to the numerical complexity to calculate the orthogonal lines, the lines are only available in the crossover region. Since the leakage flux in the aligned position is negligible, the calculated flux in SC mapping agrees closely with the finite element method (FEM) results.

To calculate the phase flux linkage as a function of the rotor position, the difference between two magnetic vector potentials located at the stator tooth contour (activated region) is considered. The phase flux linkage calculated with SC is compared to that with FEM in Figure 5. Although in general there is a good agreement, the SC values have a discrepancy where the OFD are not parallel, i.e. when the rotor and stator teeth are not aligned. According to the OFD, the magnetic potential changes linearly on the activated tooth border, having its maximum value at the nearest point to the airgap. From the energy conversion point, this is a very logical assumption since the electromagnetic energy conversion takes place in the airgap. However, in FEM, the magnetic vector potential is assumed to be constant along the source-tooth border

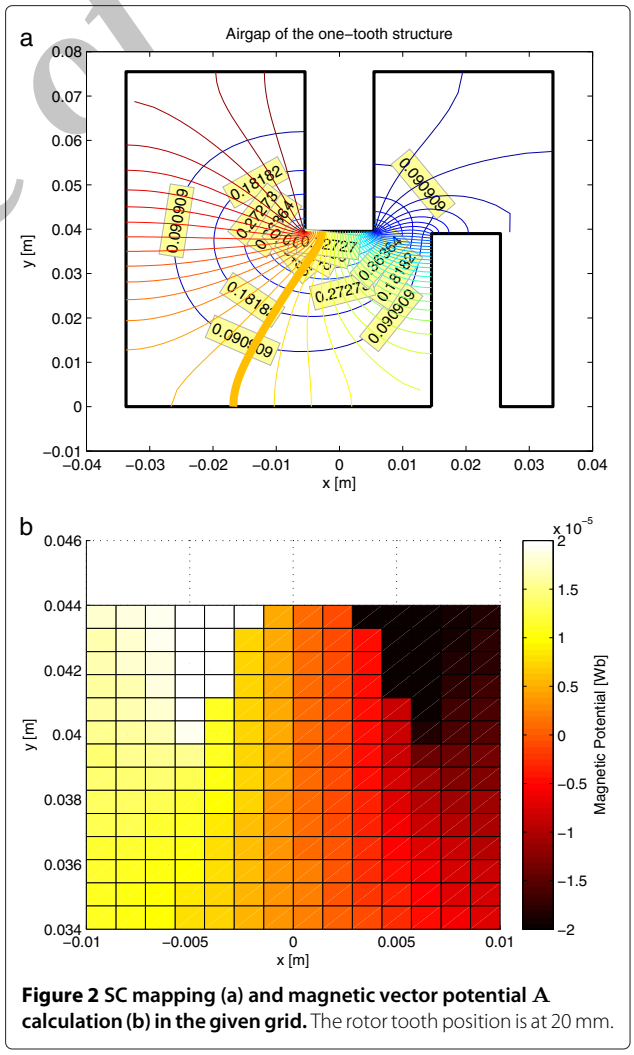

Figure 2 SC mapping (a) and magnetic vector potential A calculation (b) in the given grid. The rotor tooth position is at 20 mm.

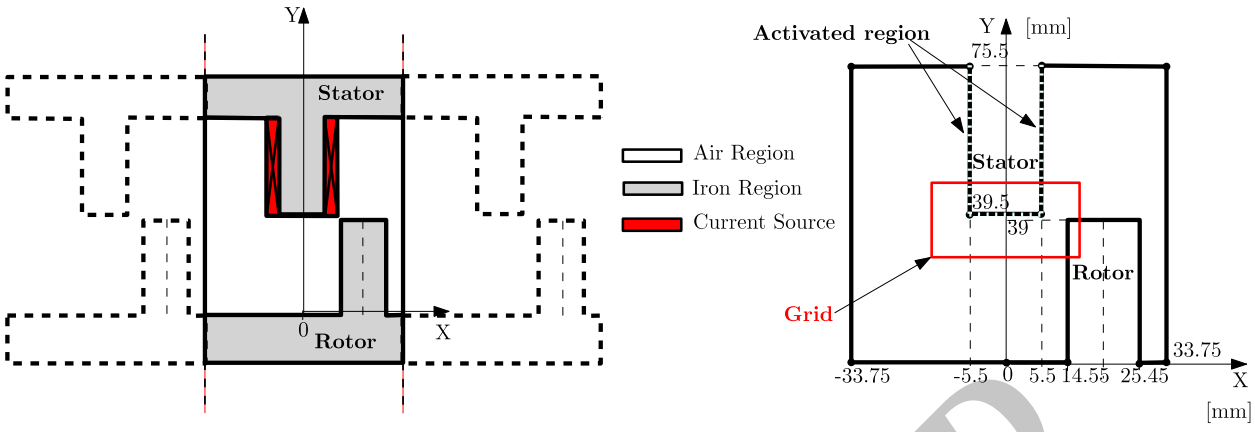

Figure 3 Double salient cell structure used in SC mapping.

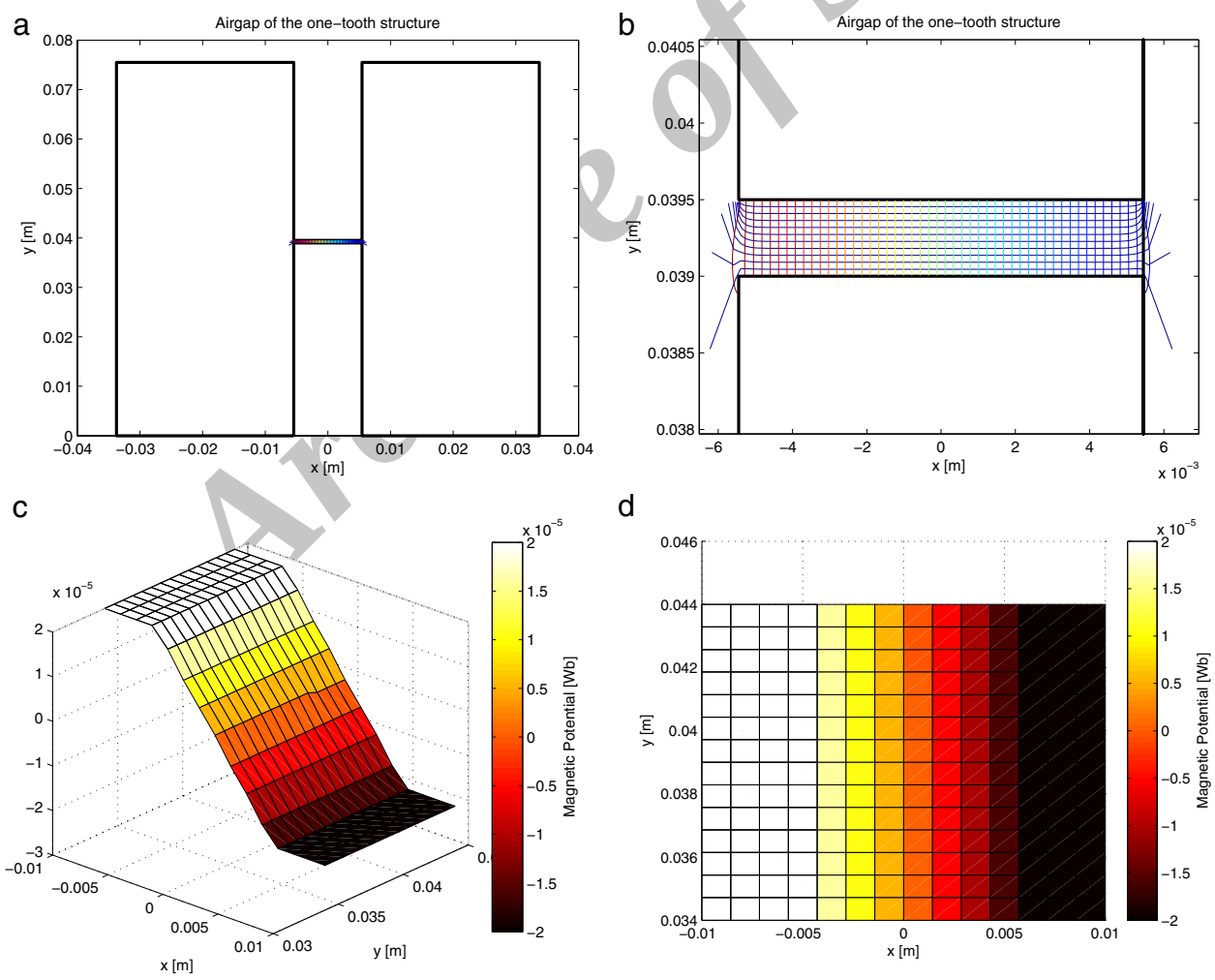

Figure 4 SC mapping (a, b), magnetic vector potential A calculation (c) in the given grid, and density plot of A (d). The rotor tooth position is at 0 mm.

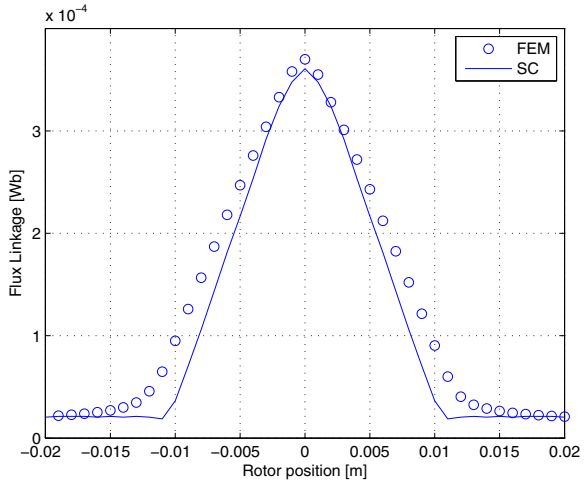

Figure 5 Comparison of phase flux linkage with SC vs. with FEM.

(contour) line. The discrepancy in Figure 5 is a result of this difference.

SC mapping with TCM on a double salient structure

In [6], how to implement the TCM for flux-switching machine is explained. To calculate the airgap and magnet-related permeances, electrostatic FEM (eFEM) is used. Although the accuracy of FEM is very good, it requires a long time for an adequate mesh and for the solving process. Additionally, the results need to be post-processed in MATLAB before the permeances are inserted in the TCM network. To overcome these problems and for a full integration into the MATLAB environment, SC mapping is used instead of FEM to calculate the airgap permeances.

In TCM, the permeances between relevant tooth contours (TCs) have to be calculated as a function of rotor position. With the SC, the permeance paths (flux paths) in the original domain are not easy to approximate. Many researchers tried approximating the flux paths with already existing permeance formulas. With the mapping function of the SC, such approximations become unnecessary. Using the *crrectmap* function in the MATLAB SC toolbox, the double salient airgap is converted into a rectangle. While using this MATLAB function, four vertices, which are the corner points of the mapped region, have to be chosen. These vertices can be any four out of the total 12 vertices in Figure 6a. These four vertices illustrate the begin- and end-points of the two TCs, which are considered for the permeance calculation in the TCM. In this structure, the first TC is chosen as the whole stator tooth between vertices 7 and 10, and the second TC can be any one of the three rotor TCs, i.e. vertices 1 to 2, 2 to 3 or 3 to 4. For example in Figure 6a, if the stator TC and the upper rotor TC (TC_2 in [6]) facing the airgap horizontally are chosen, then vertices 2, 3, 7, and 10 have to be inserted into *crrectmap* in a counterclockwise direction. The result of this permeance calculation by SC is compared to eFEM in Figure 6b, which shows only a 4% difference for the whole range of the electrical cycle. Since this result is well within the accepted limits, the SC model can be used instead of eFEM to calculate the airgap and magnet permeances.

Results and discussion

SC-TCM implementation for FSPM

This section extends the simple double salient cell structure to a FSPM cell structure for complete machine simulation. Using the symmetries and periodicities in the FSPM machine geometry, one stator cell period and one rotor tooth in Figure 7a are considered for airgap permeance calculations. In [6], while using eFEM for permeance

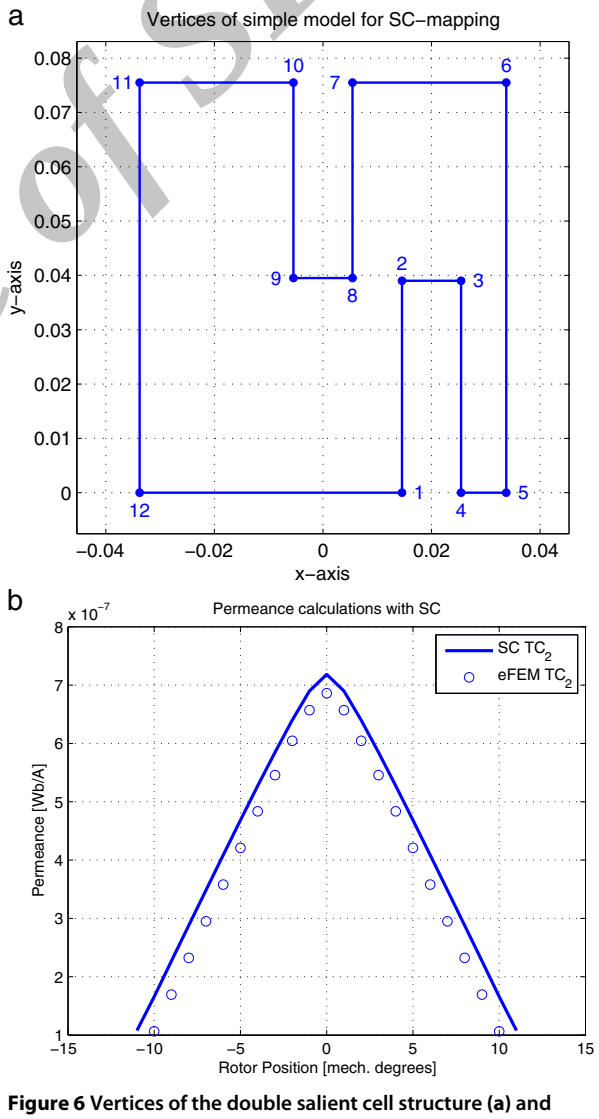

Figure 6 Vertices of the double salient cell structure (a) and comparison of airgap permeance calculation for TC_2 (b).

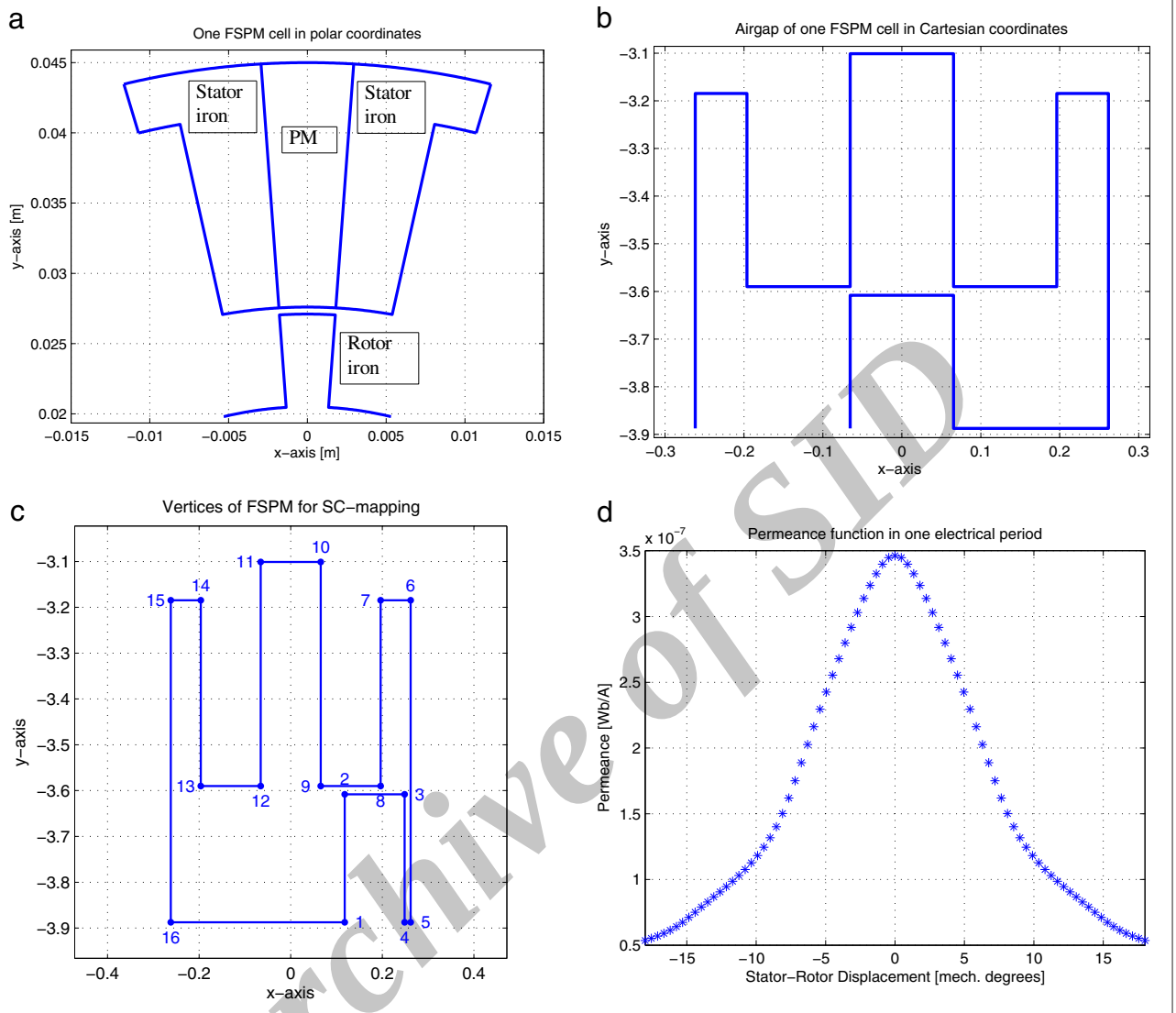

Figure 7 SC model for FSPM cell (a, b, c) and airgap permeance calculated by SC mapping (d).

calculations, the real polar geometry of the FSPM is used. Because SC mapping works only in the Cartesian coordinate system, the considered machine has to be converted from the polar to the Cartesian coordinate system, and a correction factor has to be applied after calculating the permeance to minimize the error in the permeance values. The steps for the SC-TCM integration in MATLAB are summarized as follows:

1. Create one FSPM cell in polar coordinates (Figure 7a),
2. Transform the geometry from the polar to Cartesian coordinates (using the complex log function; Figure 7b),
3. Find the polygon vertices of the SC mapping (Figure 7c),
4. Apply the *crrectmap* function in MATLAB on the corresponding vertices for each considered TC, i.e. vertices 11 to 14 to vertices 1 to 2, 2 to 3 and 3 to 4,
5. Run the previous step for half an electrical period,
6. Mirror results of step 5 for the other half of the period (Figure 7d),
7. Apply a correction factor to the airgap permeance functions (Figure 8),
8. Extrapolate the permeance values until zero permeance values are obtained,
9. Introduce the permeance values obtained in step 8 into the reluctance network of TCM.

Due to the double salient structure of the FSPM, there is a notable cogging torque, which could cause mechanical problems. For cogging torque calculation, step 8 is very

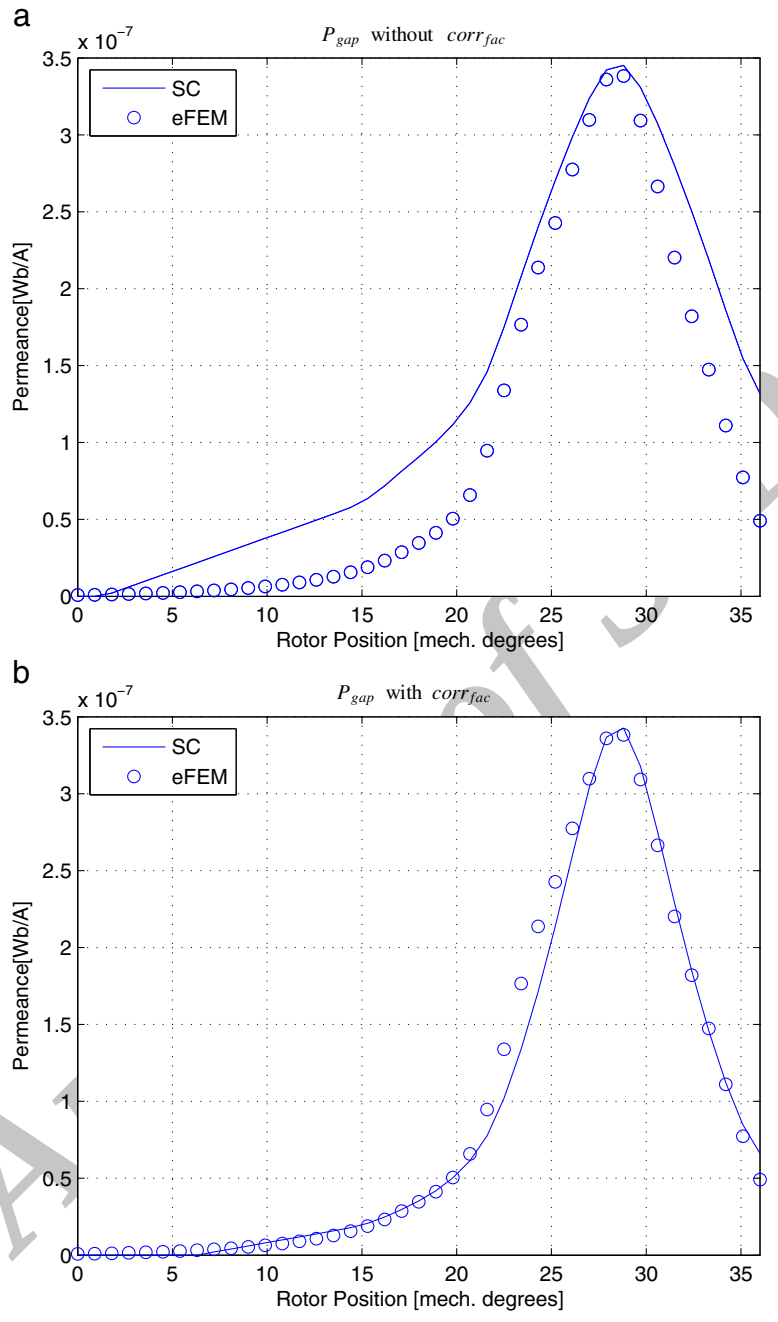

Figure 8 Comparison between SC and eFEM for airgap permeance $\mathcal{P}_{s12}$ calculation (a) without and (b) with correction factor.

important, because the accuracy of the calculation highly depends on the accuracy of the airgap permeances, even for small values.

Correction factor

Preliminary results in Figure 8a show that the permeances calculated by SC-TCM have higher values at certain rotor positions compared to the values calculated by the eFEM-TCM. Only the results at the rotor position, where the stator tooth-rotor tooth alignment commences, are identical. At the remaining rotor positions, the error percentage increases with increasing distance between the stator-rotor teeth. This result is due to the differently increasing distance in the two coordinate systems. The distance between the stator and rotor teeth in the polar coordinate system (eFEM) does not linearly increase compared to the distance in the Cartesian coordinate system (SC).

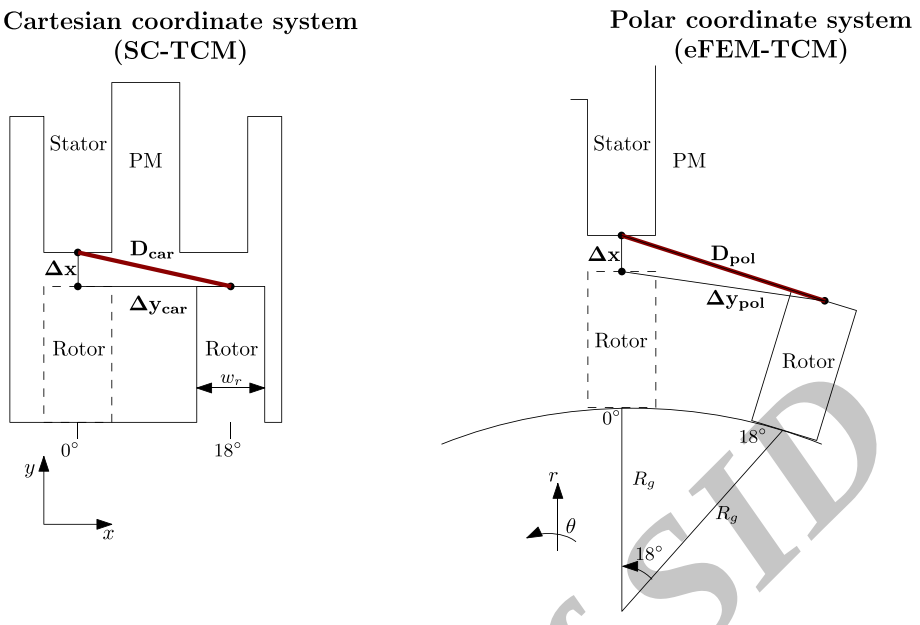

Figure 9 Calculation of the correction factor.

In order to minimize the difference between the permeances calculated by SC and eFEM, a correction factor (corr_{fac}) is implemented:

$$\text{corr}_{\text{fac}} = \frac{D_{\text{car}}}{D_{\text{pol}}}, \tag{1}$$

where D_{car} is the distance between the center of rotor-stator TCs in the Cartesian coordinate system and D_{pol} is the corresponding distance in the polar coordinate system, as shown in Figure 9. For the Cartesian coordinate system in Figure 9, w_r corresponds to 0.1309 mm in the SC coordinate system. The correction factor varies with the rotor position, i.e. depends on the y-axis position in the Cartesian coordinate system and on θ-axis position in the polar coordinate system. For consistency in the formulas, the distance calculations for both D_{car} and D_{pol} are given in the Cartesian coordinate system:

$$\begin{aligned} D_{\text{car,pol}} &= \sqrt{(\Delta x)^2 + (\Delta y)^2} \\ \Delta x &= \text{airgap} \\ \Delta y_{\text{car}} &= \frac{w_r}{7.5^\circ}[\,0^\circ : 18^\circ] \\ \Delta y_{\text{pol}} &= R_g \frac{\sin(0.5[\,0^\circ : 18^\circ])}{2}. \end{aligned} \tag{2}$$

Both D_{car} (SC-TCM) and D_{spol} (eFEM-TCM) are distances calculated for the half mechanical period $[\,0^\circ : 18^\circ]$.

SC-TCM vs. eFEM-TCM

In both modelling techniques, SC-TCM and eFEM-TCM, the rotor tooth is considered as consisting of three separate TCs. However in SC-TCM, the stator is considered as a whole TC (vertices 11 to 14), whereas in the eFEM-TCM, the stator is divided in multiple separate TCs. For each network node of the reluctance model in TCM, the separate permeances are summed up after the circuit is solved for each rotor position. Consequently, permeances calculated by SC and eFEM can be compared to each other.

Results for FSPM

Results in Figure 10 show that a highly improved TCM model is achieved by integration with the SC, compared to eFEM-TCM. The flux linkage of SC-TCM is much smoother, and the harmonic content of the cogging torque shows a higher resemblance to the FEM results.

In the 'SC-TCM vs. eFEM-TCM' section, the change in permeance calculation sequence is made to decrease the calculation time of SC-TCM and to make it comparable with eFEM-TCM. This change has no effect on the calculated quantities. The differences in Figure 10 are only due to differences in permeances. Permeance accuracy greatly affects the cogging torque calculation, which depends on the airgap and magnet permeances, i.e. on the energy stored in the airgap. Computation time by SC-TCM takes 13.2 min using only MATLAB, whereas eFEM-TCM takes 12 min using a FEM software for solving and MATLAB for post-processing.

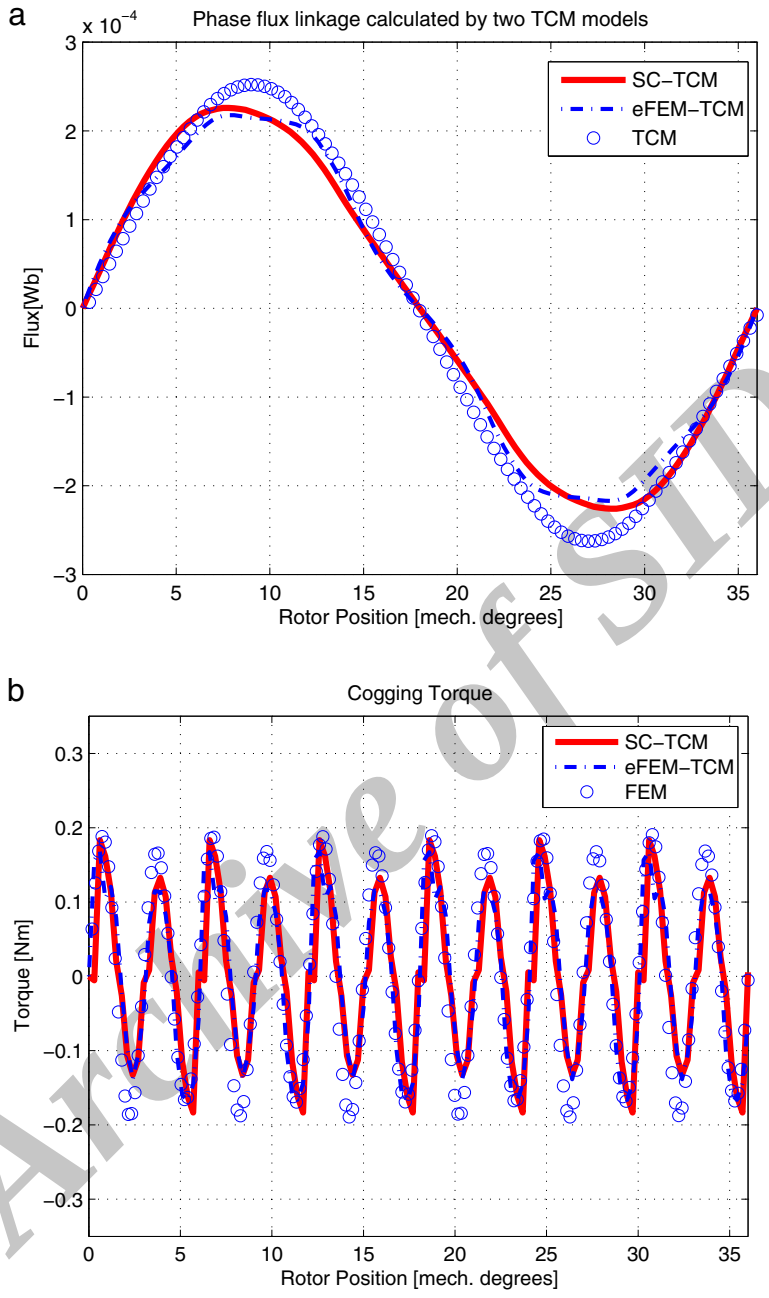

Figure 10 Comparison of phase flux linkage (a) and comparison of cogging torque of SC-TCM, eFEM-TCM and FEM (b).

Conclusions

With this research, it is shown how numerical SC mapping can be used in FSPM modelling. All relevant problems along with their solutions are discussed on the double salient machine structure of FSPM. The techniques introduced in this paper can be adapted to other machines as well.

Competing interests

The authors declare that they have no competing interests.

Authors' contributions

EI wrote the main program files necessary to compute the models. ETM, JJHP and EAL conceived of the study and participated in its design and coordination. All authors read and approved the final manuscript.

Authors' information

EI, ETM, JJHP and EAL (senior) are members of IEEE.

Acknowledgements

This project is part of the IOP-EMVT programme inside Senter-Novem, an agency of the Dutch Ministry of Economical Affairs.

Received: 10 April 2012 Accepted: 14 July 2012
Published: 18 September 2012

References

1. Kim, TH: A study on the design of an inset-permanent-magnet-type flux-reversal machine. Magnetics IEEE Trans on. **45**(6), 2859–2862 (2009)
2. Owen, R, Zhu, Z, Jewell, G: Hybrid-excited flux-switching permanent-magnet machines with iron flux bridges. Magnetics IEEE Trans on. **46**(6), 1726–1729 (2010)
3. Gysen, B, Ilhan, E, Meessen, K, Paulides, J, Lomonova, E: Modeling of flux switching permanent magnet machines with Fourier analysis. Magnetics IEEE Trans on. **46**(6), 1499–1502 (2010)
4. Huang, L, Yu, H, Hu, M, Zhao, J, Cheng, Z: A novel flux-switching permanent-magnet linear generator for wave energy extraction application. Magnetics IEEE Trans on. **47**(5), 1034–1037 (2011)
5. Ilhan, E, Gysen, B, Paulides, J, Lomonova, E: Analytical hybrid model for flux switching permanent magnet machines. Magnetics IEEE Trans on. **46**(6), 1762–1765 (2010)
6. Ilhan, E, Paulides, J, Encica, L, Lomonova, E: Tooth contour method implementation for the flux-switching pm machines. In *2010 XIX International Conference on Electrical Machines (ICEM)*, Rome, 6–8 (Sept 2010)
7. Qi, Z-s, Guo, Y, Wang, B-h: Blind direction-of-arrival estimation algorithm for conformal array antenna with respect to polarisation diversity. Microwaves, Antennas Propagation IET. **5**(4), 433–442 (2011)
8. Elnakib, A, El-Baz, A, Casanova, M, Gimel'farb, G, Switala, A: Image-based detection of corpus callosum variability for more accurate discrimination between dyslexic and normal brains. In *2010 IEEE International Symposium on Biomedical Imaging: From Nano to Macro*, Rotterdam, 14–17 (April 2010)
9. Boughrara, K, Ibtiouen, R, Zandarko, D, Touhami, O, Rezzoug, A: Magnetic field analysis of external rotor permanent-magnet synchronous motors using conformal mapping. Magnetics, IEEE Trans on. 46(9) (2010)
10. Krop, D, Lomonova, E, Vandenput, A: Application of schwarz-christoffel mapping to permanent-magnet linear motor analysis. Magnetics IEEE Trans on. **44**(3), 352–359 (2008)
11. Gysen, B, Lomonova, E, Paulides, J, Vandenput, A: Analytical and numerical techniques for solving laplace and poisson equations in a tubular permanent magnet actuator: part II. Schwarz–Christoffel mapping. Magnetics IEEE Trans on. **44**(7), 1761–1767 (2008)
12. Markovic, M, Jufer, M, Perriard, Y: Analyzing an electromechanical actuator by Schwarz–Christoffel mapping. Magnetics IEEE Trans on. **40**(4), 1858–1863 (2004)
13. Driscoll, T, Trefethen, L: Schwarz-Christoffel Mapping: Cambridge Monographs on Applied and Computational Mathematics. Cambridge University Press, Cambridge (2002)
14. Driscoll, T: Schwarz-Christoffel toolbox for MATLAB. http://www.math.udel.edu/driscoll/software/SC/index.html. Accessed August 2012

doi:10.1186/2251-7456-6-37
Cite this article as: Ilhan *et al.*: **Conformal mapping: Schwarz-Christoffel method for flux-switching PM machines.** *Mathematical Sciences* 2012 **6**:37.